2013-08-05

Investigation of Arsenic and Antimony Capping Layers, and Half Cycle Reactions During Atomic Layer Deposition of Al_2O_3 on GaSb(100)

UTD AUTHOR(S): Dmitry M. Zhemokletov, Hong Dong, Barry Brennan, Jiyoung Kim and Robert M. Wallace

JVSTA Journal of Vacuum Science & Technology A

Investigation of arsenic and antimony capping layers, and half cycle reactions during atomic layer deposition of Al2O3 on GaSb(100)

Dmitry M. Zhernokletov, Hong Dong, Barry Brennan, Jiyoung Kim, Robert M. Wallace, Michael Yakimov, Vadim Tokranov, and Serge Oktyabrsky

Citation: Journal of Vacuum Science & Technology A **31**, 060602 (2013); doi: 10.1116/1.4817496
View online: http://dx.doi.org/10.1116/1.4817496
View Table of Contents: http://scitation.aip.org/content/avs/journal/jvsta/31/6?ver=pdfcov
Published by the AVS: Science & Technology of Materials, Interfaces, and Processing

Investigation of arsenic and antimony capping layers, and half cycle reactions during atomic layer deposition of Al_2O_3 on GaSb(100)

Dmitry M. Zhernokletov
Department of Physics, University of Texas at Dallas, Richardson, Texas 75080

Hong Dong, Barry Brennan, Jiyoung Kim, and Robert M. Wallace[a)]
Department of Materials Science and Engineering, University of Texas at Dallas, Richardson, Texas 75080

Michael Yakimov, Vadim Tokranov, and Serge Oktyabrsky
College of Nanoscale Science and Engineering, University at Albany–SUNY, Albany, New York 12203

(Received 20 June 2013; accepted 19 July 2013; published 5 August 2013)

In-situ monochromatic x-ray photoelectron spectroscopy, low energy electron diffraction, ion scattering spectroscopy, and transmission electron microscopy are used to examine the GaSb(100) surfaces grown by molecular beam epitaxy after thermal desorption of a protective As or Sb layer and subsequent atomic layer deposition (ALD) of Al_2O_3. An antimony protective layer is found to be more favorable compared to an arsenic capping layer as it prevents As alloys from forming with the GaSb substrate. The evolution of oxide free GaSb/Al_2O_3 interface is investigated by "half-cycle" ALD reactions of trimethyl aluminum and deionized water. © *2013 American Vacuum Society*. [http://dx.doi.org/10.1116/1.4817496]

I. INTRODUCTION

Continued scaling with alternative channel materials shows promise in achieving low power operation and high speed switching for future complementary metal–oxide–semiconductor (CMOS) field effect transistors (FETs). Among the materials for p-MOS, GaSb is a possible candidate due to its high density of valence band states, low carrier effective masses, and high injection velocities.[1,2] One of the major obstacles to realizing field effect devices on GaSb is achieving a high quality interface with a scaled gate dielectric. During *ex situ* device processing GaSb readily oxidizes before high-k gate oxide deposition due to atmospheric exposure, resulting in the formation of a relatively thick native oxide layer, which can lead to interface trap states and Fermi level pinning.[2] Engineering devices of superior quality on GaSb has to address the surface properties of this material. Recent studies on the integration of high-κ dielectrics on GaSb have primarily focused on the use of thermal atomic layer deposition (ALD)[3,4] and Plasma Enhanced ALD (PEALD).[5] Chemical pretreatments such as HCl, NH_4OH, and $(NH_4)_2S$, aiming to decrease native oxides and passivate the surface[6] followed by ALD processing, have been shown to provide high-k/GaSb structures with better interface quality.[3,4,7] In order to avoid undesirable oxidized interfacial layer formation, high-k oxide deposition directly on oxide-free GaSb surface may be more beneficial. Thermal desorption of sacrificial oxides,[8] hydrogen plasma,[9,10] or atomic hydrogen treatment[11] can be used to remove surface oxides on III-V compounds. However, these desorption methods are rather problematic since they require temperatures close to decomposition conditions of antimonides.[12] Typically, this should be done under As or Sb overpressure to avoid formation of Ga-rich surface but can result in increased surface roughness having high density of pits, which may degrade device performance.[13] Therefore, molecular beam epitaxy (MBE) followed by a metal capping/decapping procedure would be an attractive surface preparation technique, due to its potential to allow *in situ* control of the GaSb starting surface inhibiting undesirable interfacial layer formation from oxidation, subsequent high-k dielectric deposition, and control of the interface between both materials at the atomic scale.[14,15] Additionally, this amorphous group V capping layer prevents the surface from deleterious contamination and, potentially, the decapping procedure can be carried out in ALD reactor conditions. In this context, we compare arsenic and antimony capping procedures as a technique to preserve GaSb from oxidation and regenerate original stoichiometry. The quality of the As/Sb decapped GaSb surfaces was examined using low energy electron diffraction (LEED), x-ray photoelectron spectroscopy (XPS), and ion scattering spectroscopy (ISS). After decapping, *in situ* ALD of Al_2O_3 was performed on the reconstructed GaSb(100) surfaces, with XPS and transmission electron microscopy (TEM) were used to characterize the Al_2O_3/GaSb interface both chemically and structurally.

II. EXPERIMENT

MBE was employed to grow a 1 μm thick Te-doped GaSb(100) layers on lattice matched $Al_{0.7}Ga_{0.3}As_{0.07}Sb_{0.93}$ metamorphic buffer layers on top of n-GaAs(001) substrates. After the growth, an amorphous arsenic or antimony cap layer (~175 nm thick) was deposited at room temperature on top of the GaSb surface. Both samples were then mounted to separate sample holders and introduced into a multifunctional deposition/characterization ultrahigh vacuum (UHV) system described elsewhere.[16] The complete desorption of the protective capping layers was obtained in a chamber with a base pressure of 1×10^{-10} mbar by annealing the As capped sample at 400 °C for 30 min[17] with the appearance of a streaky (2×3) GaSb(100) reconstructed surface,[18] while

[a)]Electronic mail: rmwallace@utdallas.edu

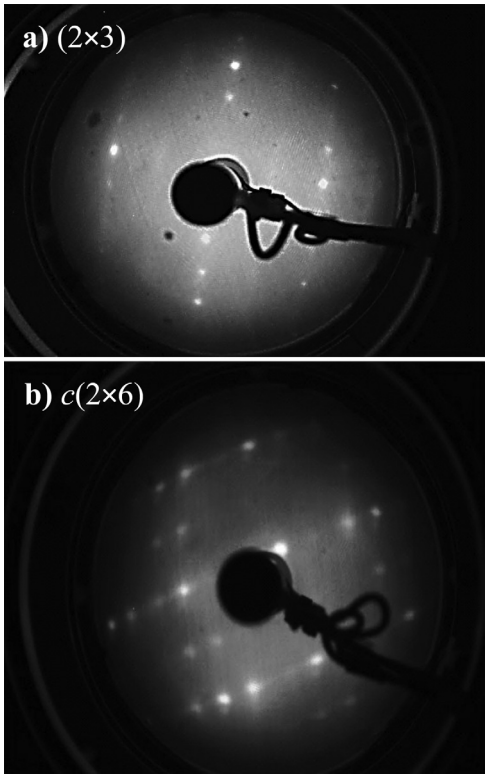

FIG. 1. LEED pattern from the GaSb(100) surface: (a) 2×3 at 73 eV after As capping layer removal, (b) $c(2 \times 6)$ at 73 eV after Sb capping layer removal.

the Sb capping layer was thermally desorbed at 300 °C for 30 min, which resulted in $c(2 \times 6)$ GaSb(001) LEED pattern formation.[19] In order to characterize the chemical makeup of the very top 1–2 monolayers of the decapped GaSb surface, ISS[20] was performed using 1 keV He^+ ions.

The samples were interrogated by monochromatic, *in-situ* XPS, using an Al Kα source emitting photons with an energy of 1486.7 eV, to determine whether the different capping layers impacted the chemistry of the GaSb surface and to ensure no oxide was present. This further served as a control spectrum to establish the XPS core level line shapes for the atomically clean surface, to facilitate the careful spectral deconvolution procedure conducted here.[21,22] XPS spectra were taken at 45° (surface sensitive) and 75° (bulk sensitive) take-off angles measured with respect to the surface plane. After the XPS scan of the decapped surfaces, photoelectron spectra were acquired after each of: (1) heating at 300 °C inside the ALD reactor vacuum ambient ($P \approx 10^{-2}$ mbar) for 30 min, (2) 1st pulse trimethyl aluminum (TMA) exposure, (3) 1st pulse deionized water (DIW) exposure, (4) 5 cycles of Al_2O_3, (5) 10 cycles of Al_2O_3, and (6) finally after 20 cycles of Al_2O_3 (all performed at 300 °C). The pulse duration for both TMA and DIW was 0.1 s followed by a 4 s N_2 purge after each pulse, with the total pressure during ALD of $P \sim 9$ mbar. Upon ALD oxide formation, the peak positions were aligned such that the bulk peaks would appear at the same binding energy as the reference Sb-decapped GaSb(100) surface in order to correct for band bending and surface charging effects.[23] Spectral peaks were deconvoluted with the software tool AANALYZER,[24] using Voigt functions with independent control of the Lorentzian and Gaussian components. A dynamic Shirley background is used for all fits, which allows for modifications to the background during the fitting process to give a more accurate background line shape.[25]

III. RESULTS AND DISCUSSION

With the arsenic decapping procedure being carried out at 400 °C, a (2×3) surface reconstruction is observed on the GaSb, where each row of diffraction spots is separated by one less well-resolved diffraction streak [as shown in Fig. 1(a)]. This reconstruction corresponds to an Ga-rich surface, consisting of Ga atomic rows on the surface.[6] The Sb decapping procedure carried out at 300 °C reveals an GaSb(100)-$c(2 \times 6)$ LEED pattern [Fig. 1(b)], which is attributed to an Sb-rich regime with Sb-Sb dimer chains on the surface.[26]

The As 3*d* spectrum of the arsenic capped GaSb [Fig. 2(a)] surface shows peaks at 41.6 and 44.9 eV, which are attributed to elemental arsenic from the cap and arsenic oxides on the surface of the cap, respectively. The presence of these arsenic oxides indicates that the top surface of the arsenic cap is not inert to air oxidation with an exposure time of about 5 days, suggesting that a sufficiently thick layer is needed to prevent complete oxidation. Heating the As-capped GaSb sample to 400 °C eliminates the As 3*d* peak at 41.6 eV, revealing a new As 3*d* feature at 41.1 eV, which

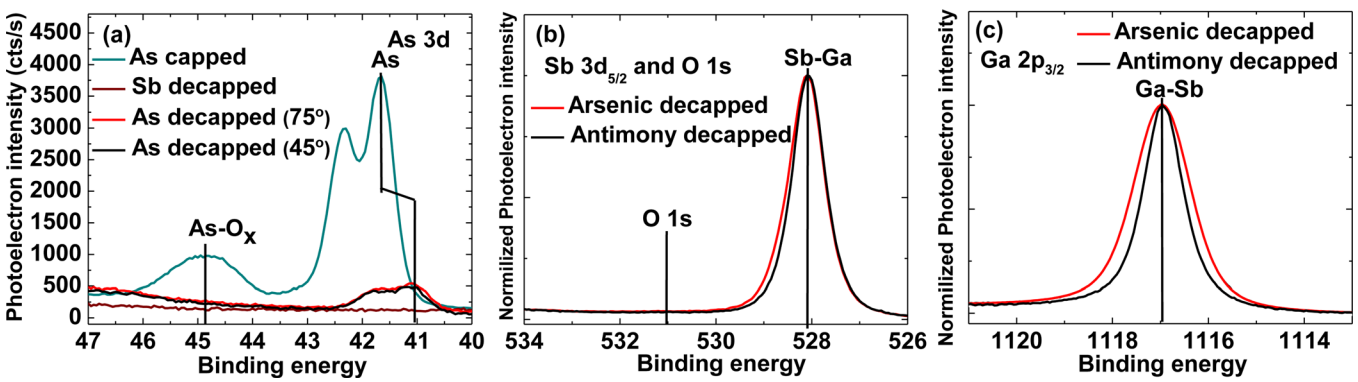

FIG. 2. (Color online) XPS spectra of (a) As 3*d*, (b) O1*s* and Sb3*d*, and (c) Ga2*p* core level spectra for As capped, Sb decapped, and As-decapped for 45° and 75° take-off angles.

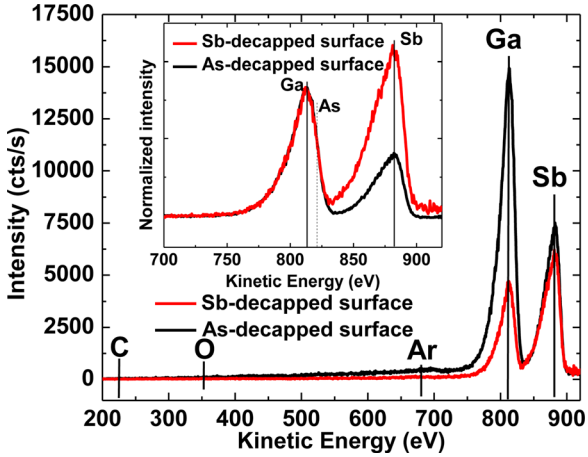

FIG. 3. (Color online) ISS spectra for As and Sb-decapped surfaces, recordered for 1 kEv He^+ beam incident at an angle of 72° relative to the surface plane with 143° scattering angle. The peaks at 810 and 880 eV result from scattering by gallium and antimony atoms, respectively. Inset shows ISS spectra normalized to the same height at maximum gallium intensity.

can be assigned to the arsenic bonded to the GaSb surface. The fact that the As 3*d* signal significantly decreases upon decapping and does not show any angular dependence suggests that this arsenic layer is homogeneously distributed at the interface, and confirmed by ISS measurements (see below). As expected, no traces of arsenic are detected on the Sb-decapped surface.

Figure 2(b) presents the Sb $3d_{5/2}$ and O 1*s* core level spectra after the As and Sb-decapping procedure. Upon capping layer removal, the O 1*s* feature is below the XPS detection limit on both samples suggesting that both As and Sb metals are effective at preserving the MBE-grown GaSb surfaces from air oxidation. The broader peak width of the Sb $3d_{5/2}$ and Ga $2p_{3/2}$ [Fig. 2(c)] features detected on the As-decapped surface suggests that the residual arsenic (~7 at. %) is possibly alloyed with gallium and antimony. In fact, both the As:Ga and As:Sb ratios calculated from the data taken at take-off angles of $\theta = 45°$ and $\theta = 75°$ (without taking into account the atomic sensitivity factors) increase by ~8%, with higher arsenic concentration detected in the bulk sensitive measurement. The estimated surface composition calculated at $\theta = 45°$ take-off angle using atomic sensitivity factors is $Ga_{0.5}Sb_{0.5}$ for the Sb-decapped surface and $Ga_{0.52}Sb_{0.41}As_{0.07}$ for the As-decapped. Therefore, it is plausible that a thin layer of GaAsSb is introduced on the GaSb surface by the arsenic decapping procedure.

Figure 3 shows ISS spectra collected from As and Sb-decapped surfaces at a detection angle of 72° relative to the surface plane, with a 143° scattering angle. Both surfaces contain no detectable oxygen or carbon. The antimony peak intensities located (at ~880 eV) are almost identical for the As and Sb-decapped surfaces; however, the gallium signal intensity (at ~810 eV) is much stronger for the As-decapped surface. In fact, after taking into account the ISS sensitivity factors[20] the calculated ratios of Ga:Sb appear to be 4:1 for the As-decapped surface and 2:3 for Sb-decapped surface, suggesting that the higher As-decapping temperature leads to a Ga-rich surface. No arsenic atoms are detected on As-decapped surface, as shown in the inset of Fig. 3. Since arsenic and gallium atomic masses are close to each other (69.7 and 74 amu), an arsenic feature (at ~823 eV) would result in the broadening of the peak assigned to the Ga

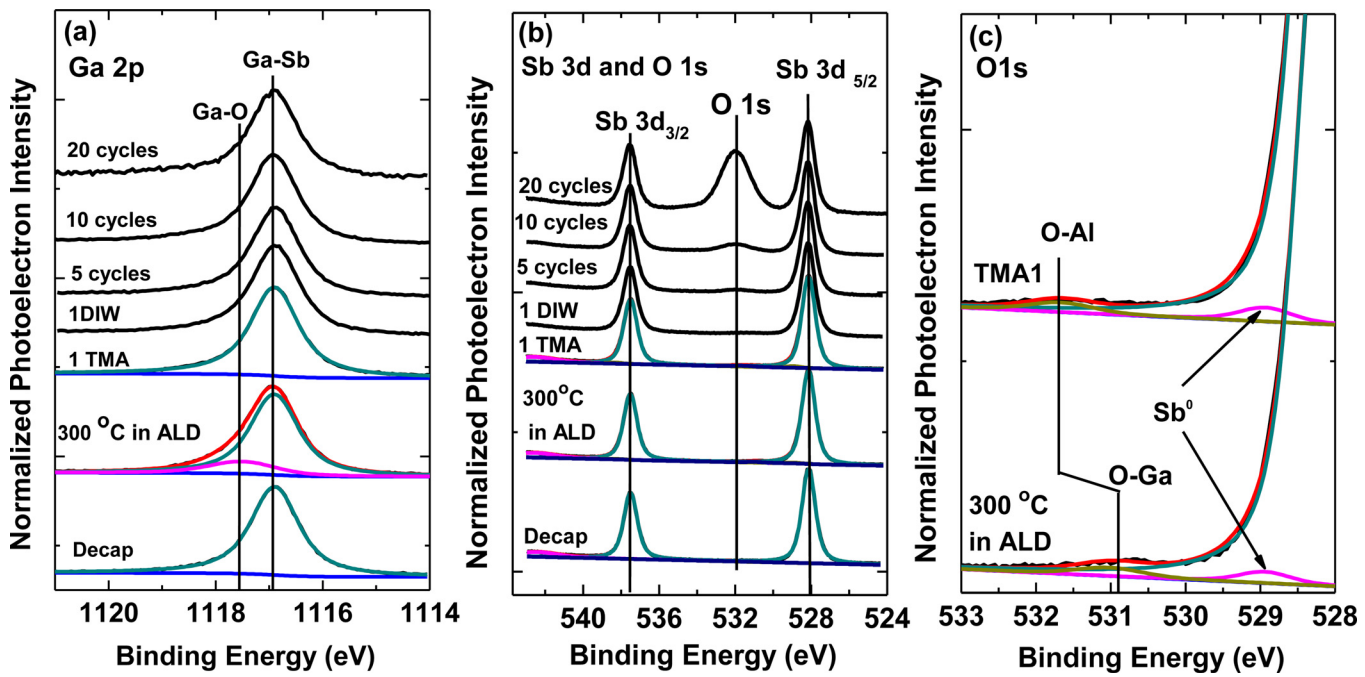

FIG. 4. (Color online) (a) Ga 2*p* and (b) Sb 3*d* and O 1*s* XPS spectra showing chemical state evolution after the decapping procedure, 300 °C heat treatment and the first TMA pulse. The raw spectra after each of the following: 1st pulse of DIW exposure, 5 and 10 cycles, and finally after 20 full cycles of Al_2O_3 deposition are also included, however spectral analysis shows no changes other than attenuation. (c) O 1*s* XPS spectra before and after the first pulse of TMA showing chemical shift associated with O-Al bond formation.

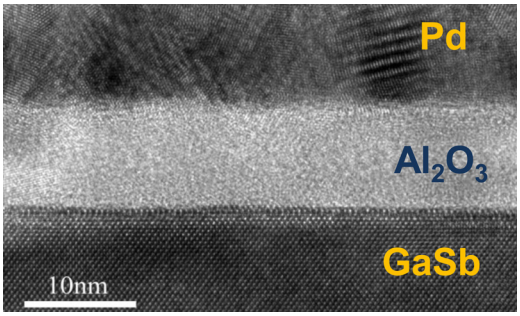

FIG. 5. (Color online) TEM picture of an Al_2O_3/GaSb(100) heterostructure showing an abrupt interface.

feature, however, the gallium peak width obtained from As-decapped surface corresponds to the same gallium peak width obtained on Sb-decapped surface. This suggests that Sb diffuses to the surface during As-decapping procedure which is most likely due to the binding energy difference between GaAs and GaSb binary systems.[27] In the case of GaAsSb, GaAs binary system has higher binding energy than GaSb, which results in a lower kinetic barrier to Sb segregation.[28]

Since we showed that the Sb capping layer produces a chemically clean starting surface compared to As capping, we use this to investigate the interfacial chemistry of Al_2O_3 ALD directly on the Sb-decapped surface. Figure 4(a) shows the evolution of the surface sensitive[29] Ga $2p_{3/2}$ and Sb $3d$ spectra, (which overlaps with the O $1s$ feature at ~532 eV), after sequential TMA and H_2O precursor pulses. The antimony region, due to the lower binding energy of the core level (higher kinetic energy of electron), is not as surface sensitive as the gallium $2p$ spectra shown here; however, it is the most surface sensitive core level available using an Al Kα x-ray source.

As previously discussed, the surface shows evidence of only Ga–Sb bonds following thermal desorption of the Sb capping layer and the O $1s$ core level signal is below the level of detection and is referred to herein as an "oxide-free" surface. Prior to the first TMA exposure the sample is inserted into the ALD reactor for 30 min at 300 °C in order to determine the effect of reactor conditions during deposition. This exposure to the ALD reactor was maintained at ~9 mbar, and results in Ga-O state formation offset by 0.6 eV from the bulk peak, consistent with the binding energy of Ga_2O.[14] At the same time, a signal in the O $1s$ spectra is detected at ~530.9 eV [Figs. 4(b) and 4(c)], which is also consistent with O-Ga bonding. Since the binding energies of the oxidation states of Sb $3d_{3/2}$ overlap with O $1s$ features, this assignment is made based on the fact that no oxidation states are detected in Sb $3d_{3/2}$ spectra [Fig. 4(a)], which would also be observed in Sb $3d_{5/2}$ spectra.

The first TMA pulse decreases signal from Ga-O state below XPS detection limits. This transfer of oxygen from O-Ga to O-Al bonding is illustrated in the O $1s$ region in Fig. 4(c) as the peak is observed to shift to a higher binding energy of ~531.7 eV, associated with Al–O formation, with no antimony oxidation states detected [Fig. 4(b)]. This suggests that the connection between the oxide free GaSb substrate and Al_2O_3 takes place through Ga-O-Al interfacial bonds via a ligand exchange mechanism.[30] A LEED pattern was no longer observed after the initial pulse of TMA, indicating that the formed overlayer is amorphous. The GaSb/Al_2O_3 interface appears chemically stable as, following further twenty pulses of TMA and water, the chemical configuration of Al_2O_3/GaSb interface is not significantly affected.

A high resolution cross-sectional transmission electron microscopy (HRTEM) image in Fig. 5 taken along the $\langle 110 \rangle_{GaSb}$ direction shows the structural quality of the Al_2O_3/GaSb interface. The completely amorphous Al_2O_3 thin film without any crystallites in the layer, presents a uniform thickness of 7.3 ± 0.2 nm after 100 cycles of TMA and H_2O and a flat surface between dielectric and semiconductor. The Al_2O_3/GaSb interface is sharp and continuous with no interfacial layer observed. The TEM image reveals the good homogeneity of the stack, and the absence of interfacial defects like pinholes or pits on the GaSb surface which could have been caused by the initial ALD steps. The density of threading dislocations in the GaSb epilayer were at high 10^7-low 10^8 cm^{-2} level as found from low-magnification TEM analysis.[31]

IV. CONCLUSION

In conclusion, our experimental results confirm that the arsenic and antimony capping/decapping technique is appropriate for preservation of the GaSb surface from oxidation. However, the As capping technique does not regenerate stoichiometric GaSb upon cap removal due to alloying of residual arsenic with the substrate during thermal desorption. Well-controlled *in situ* surface preparation of GaSb and atomic layer deposition of Al_2O_3 results in efficient passivation, with an abrupt oxide/semiconductor interface and no Sb or Ga oxides detected by XPS. The initial growth mechanism involves Ga-O bond formation in the ALD reactor environment, this state is scavenged by subsequent TMA exposure, which clearly shows interaction between the TMA molecule and Ga oxidation states through the "clean-up" effect.

ACKNOWLEDGMENTS

The authors would like to thank S. McDonnell and C. L. Hinkle (UT Dallas) for the useful discussions. This work was supported by the Semiconductor Research Corporation FCRP Materials Structures and Devices (MSD) Center the Nanoelectronics Research Initiative and the National Institute of Standards and Technology (NIST) through the Midwest Institute for Nanoelectronics Discovery (MIND), and the National Science Foundation (NSF) under ECCS-0925844 and DMR-1006253 Awards.

[1]S. Oktyabrsky, in *Fundamentals of Compound Semiconductor MOSFETs*, edited by S. Oktyabrsky and P. Ye (Springer, New York, 2010), pp. 349–378.
[2]A. Nainani *et al.*, Tech. Dig. - Int. Electron Devices Meet. **2010**, 138.
[3]A. Nainani, Y. Sun, T. Irisawa, Z. Yuan, M. Kobayashi, P. Pianetta, B. R. Bennett, J. B. Boos, and K. C. Saraswat, J. Appl. Phys. **109**, 114908 (2011).

[4]M. Xu, R. Wang, and P. D. Ye, IEEE Electron Device Lett. **32**, 883 (2011).
[5]A. Ali *et al.*, Appl. Phys. Lett. **97**, 143502 (2010).
[6]D. M. Zhernokletov, H. Dong, B. Brennan, M. Yakimov, V. Tokranov, S. Oktyabrsky, J. Kim, and R. M. Wallace, Appl. Phys. Lett. **102**, 131602 (2013).
[7]D. M. Murape, N. Eassa, J. H. Neethling, R. Betz, E. Coetsee, H. C. Swart, J. R. Botha, and A. Venter, Appl. Surf. Sci. **258**, 6753 (2012).
[8]S. Ingrey, W. M. Lau, and N. S. McIntyre, J. Vac. Sci. Technol. A **4**, 984 (1986).
[9]R. P. H. Chang, C. C. Chang, and S. Darack, J. Vac. Sci. Technol. **20**, 45 (1982).
[10]J. H. Thomas III, G. Kaganowicz, and J. W. Robinson, J. Electrochem. Soc. **135**, 1201 (1988)
[11]S. Sugata, A. Takamori, N. Takado, K. Asakawa, E. Miyauchi, and H. Hashimoto, J. Vac. Sci. Technol. B **6**, 1087 (1988).
[12]P. S. Dutta, H. L. Bhat, and V. Kumar, J. Appl. Phys. **81**, 5821 (1997).
[13]K. Lee, K. Doyle, J. Chai, J. H. Dinan, and T. H. Myers, J. Electron. Mater. **41**, 2799 (2012).
[14]Y. C. Chang *et al.*, Appl. Phys. Lett. **97**, 112901 (2010).
[15]Y. H. Chang *et al.*, Appl. Phys. Lett. **101**, 172104 (2012).
[16]R. M. Wallace, ECS Trans. **16**, 255 (2008).
[17]C. Merckling, X. Sun, A. Alian, G. Brammertz, V. V. Afanas'ev, T. Y. Hoffmann, M. Heyns, M. Caymax, and J. Dekoster, J. Appl. Phys. **109**, 073719 (2011).
[18]F. Maeda, Y. Watanabe, and M. Oshima, J. Electron Spectrosc. Relat. Phenom. **80**, 225 (1996).
[19]M. Dumas, M. Nouaoura, N. Bertru, L. Lassabatère, W. Chen, and A. Kahn, Surf. Sci. **262**, L91 (1992).
[20]D. G. Swartzfager, Anal. Chem. **56**, 55 (1984).
[21]C. L. Hinkle, M. Milojevic, B. Brennan, A. M. Sonnet, F. S. Aguirre-Tostado, G. J. Hughes, E. M. Vogel, and R. M. Wallace, Appl. Phys. Lett. **94**, 162101 (2009).
[22]C. L. Hinkle, M. Milojevic, A. M. Sonnet, H. C. Kim, J. Kim, E. M. Vogel, and R. M. Wallace, ECS Trans. **19**, 387 (2009).
[23]F. S. Aguirre-Tostado *et al.*, Appl. Phys. Lett. **93**, 061907 (2008).
[24]A. Herrera-Gomez, aherrera@qro.cinvestav.mx, CINVESTAV Queretaro, Mexico.
[25]A. Herrera-Gomez, P. Pianetta, D. Marshall, E. Nelson, and W. E. Spicer, Phys. Rev. B **61**, 12988 (2000).
[26]C. Hogan, R. Magri, and R. D. Sole, Phys. Status Solidi B **247**, 1960 (2010).
[27]X. Wallart, S. Godey, Y. Douvry, and L. Desplanque, Appl. Phys. Lett. **93**, 123119 (2008).
[28]O. Dehaese, X. Wallart, and F. Mollot, Appl. Phys. Lett. **66**, 52 (1995).
[29]C. L. Hinkle, M. Milojevic, E. M. Vogel, and R. M. Wallace, Appl. Phys. Lett. **95**, 151905 (2009).
[30]B. Brennan, M. Milojevic, R. Contreras-Guerrero, H.-C. Kim, M. Lopez-Lopez, J. Kim, and R. M. Wallace, J. Vac. Sci. Technol. B **30**, 04E104 (2012).
[31]V. Tokranov, P. Nagaiah, M. Yakimov, R. J. Matyi, and S. Oktyabrsky, J. Cryst. Growth **323**, 35 (2011).